Biochimica et Biophysica Acta, 1108 (1992) 190–200

BBAMEM 75709

Cis-allosteric effects of cytoplasmic Na^+/K^+ discrimination at varying pH. Low-affinity multisite inhibition of cytoplasmic K^+ in reconstituted Na^+/K^+-ATPase engaged in uncoupled Na^+-efflux

Flemming Cornelius

Institute of Biophysics, University of Aarhus, Aarhus (Denmark)

(Received 13 December 1991)

Key words: ATPase, Na^+/K^+-; Cytoplasmic sodium activation; Cytoplasmic potassium inhibition; Potassium ion, cytoplasmic; Allosteric effect; Sodium ion-sodium ion exchange

In liposomes with reconstituted shark Na^+/K^+-ATPase the effect of cytoplasmic K^+ was investigated in the absence of extracellular alkali ions. During such conditions the Na^+/K^+-ATPase is engaged in the so called uncoupled Na^+ efflux mode in which cytoplasmic Na^+ activates and binds to the enzyme and becomes translocated without countertransport of K^+ as in the physiological Na^+/K^+ exchange mode. In this uncoupled flux mode only low-affinity inhibition by K^+_{cyt} is found to be present. The inhibition pattern is consistent with a model in which cytoplasmic K^+ exhibit mixed inhibition of Na^+ activation, probably by binding at the three cytoplasmic loading sites on E_1ATP (E_1A). With determined intrinsic binding constants for cytoplasmic Na^+ to this form of K_{S1}, K_{S2}, K_{S3} = 40 mM, 2 mM, 2 mM the inhibition pattern can be simulated assuming three K^+_{cyt} sites with equal affinity for K_I = 40 mM, similar to K_{S1} for the first Na^+_{cyt} site. The discrimination between cytoplasmic Na^+ and K^+ is therefore enhanced by allosteric interaction initiated from the *cis*-side due to binding of the first Na^+, as opposed to K^+, which induces the positive cooperativity in the successive Na^+ bindings. pH is found to influence the pattern of K^+_{cyt} inhibition. A lowering of the pH potentiates the K^+_{cyt} inhibition, whereas at increased pH the inhibition is decreased and transformed into a pure competitive competition.

Introduction

A fundamental and unresolved property of the Na^+/K^+-ATPase is its ability to discriminate among Na^+ and K^+. In order to examine this cation selectivity, investigations of the inhibition pattern of cytoplasmic K^+ on cytoplasmic Na^+ activation were performed using reconstituted shark Na^+/K^+-ATPase in the absence of extracellular cations, i.e. during the uncoupled Na^+ efflux mode [1–7]. In this flux-mode no extracellular alkali cations are occluded following dephosphorylation, and the binding sites of the enzyme returns without occlusion, with occluded empty sites, or maybe with occluded H^+. This flux mode which is one of several partial reactions the Na^+/K^+-ATPase can accommodate [8,9] is especially suited to study the ion interaction on cytoplasmic binding sites on E_1 since no interactions from extracellular ions are present, and the high-affinity K^+_{cyt} inhibition previously found [10] is absent. Both could be a problem in previous studies of cytoplasmic Na^+–K^+ interaction using red cells in which random binding of cytoplasmic Na^+ and K^+ to three equivalent sites on the E_1 form of the enzyme was suggested [11,12].

The Na^+/K^+-ATPase is inhibited by cytoplasmic K^+ at both high-affinity and low-affinity sites as suggested from experiments on unsided preparations of Na^+/K^+-ATPase [13,14] and as demonstrated in several studies using sided preparations of Na^+/K^+-ATPase [10,15,16]. In the present investigation it is found that in the absence of extracellular alkali cations the high-affinity inhibition by cytoplasmic K^+ is absent, and only a low-affinity inhibition persists. The inhibition pattern is of the multisite mixed type, where K^+_{cyt} binds both competitively with Na^+_{cyt} to an empty enzyme form and uncompetitively to an enzyme species, E_1A, with bound Na^+_{cyt}. The cation selectivity of the Na^+/K^+-ATPase appears to depend on the ability of Na^+ to induce the positive cooperativity in binding. The interplay between the three cytoplasmic binding sites on E_1A is affected by pH in a way compatible with a previous suggestion that cytoplasmic pH affects the intrinsic site dissociation constants for binding in the E_1A-pool [6].

Correspondence to: F. Cornelius, Institute of Biophysics, University of Aarhus, DK-8000, Aarhus C, Denmark.

Materials and Methods

The Na^+/K^+-ATPase used is from salt glands of the spiny dogfish, *Squalus acanthias*. The methods for preparing the membrane bound enzyme, solubilized enzyme, and its reconstitution into liposomes have been described in previous papers [17,18]. In order to study uncoupled Na^+ efflux the proteoliposomes were prepared to contain no alkali cations and in order to balance osmotically the external NaCl an equivalent amount of sucrose was included internally (260 mM). The Na^+/Na^+ exchange was studied in proteoliposomes containing 130 mM Na^+. In some experiments the internal sucrose was replaced isosmotically by TrisCl. The term efflux refers to the cellular situation and when studied on inside out incorporated Na^+/K^+-ATPase molecules, it is equivalent to an influx into the proteoliposomes. For each of the proteoliposome preparations the fraction of the enzyme molecules oriented inside-out (i:o), right-side-out (r:o), and as non-oriented (n-o) was determined by functional tests as previously described [17]. Typically, there was 15% inside-out, 65% right-side-out and 20% non-oriented.

The non-oriented enzyme molecules were inhibited by preincubation of the samples with 1 mM ouabain in the presence of 5 mM Mg^{2+} and 1 mM inorganic phosphate for 20 min at 20°C, pH 7.0 [18]. The inside-out molecules were activated by addition of ATP in the presence of the proper ligands and 1 mM ouabain. Under these conditions the non-oriented and the right-side-out molecules were inactive.

The intensity of uncoupled Na^+ efflux as well as Na^+/Na^+ exchange on i:o enzyme were assayed by measurements of the accompanying hydrolytic activity as previously described [18]. The assay period was kept below 20 s during which the rate of hydrolysis was constant. All measurements were performed at room temperature.

The specific hydrolytic activity for Na^+/K^+ exchange of the reconstituted enzyme (with the liposomes made permeable by a low concentration of detergent) was 600–900 μmol P_i/mg protein per h with Na^+ 130 mM, K^+ 20 mM, Mg^{2+} 4 mM, ATP 3 mM, 30 mM histidine, pH 7.0, 20°C.

The hydrolytic activity of the two reactions on sided preparations was as follows: ATP hydrolysis accompanying uncoupled Na^+ efflux amounted to 40–60 μmol P_i/mg protein per h with 130 mM NaCl, 2 mM $MgCl_2$, 25 μM ATP, and 30 mM histidine at the cytoplasmic side and 260 mM sucrose, 2 mM $MgCl_2$, 30 mM histidine at the extracellular side at pH 7.0, 20°C. For ATP hydrolysis accompanying Na^+/Na^+ exchange with Na^+ replacing sucrose at the extracellular side it amounted to 60–190 μmol/mg protein per h.

Results

During uncoupled Na^+ efflux mode the maximum turnover is between 5 and 10% of maximum Na^+/K^+

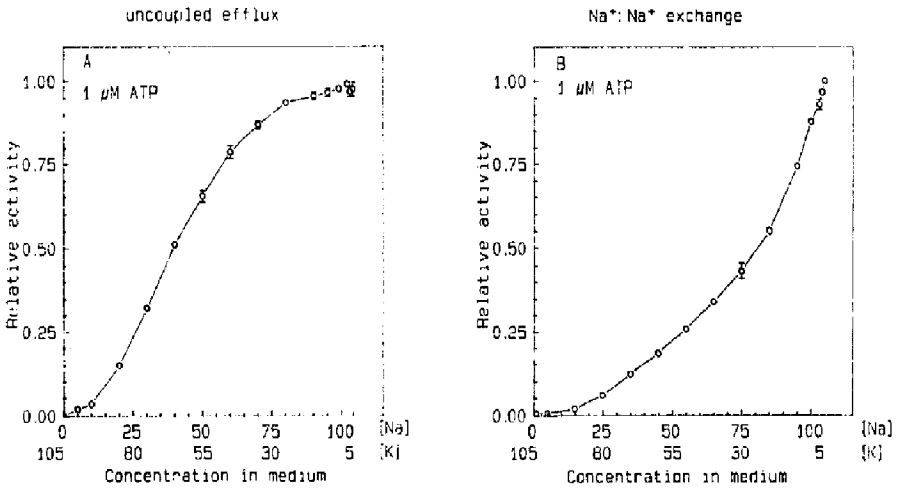

Fig. 1. Activation by inversely varied cytoplasmic concentrations of Na^+ and K^+ of ATP hydrolysis (given in relative units) at 1 μM ATP accompanying (A) uncoupled Na^+ efflux (100% equals 43 μmol/mg per h) and (B) Na^+/Na^+ exchange (100% equals 55 μmol/mg per h). Proteoliposomes contain either 260 mM sucrose (uncoupled Na^+ efflux) or 130 mM NaCl (Na^+/Na^+ exchange) besides 30 mM histidine (pH 7.0) and 2 mM Mg^{2+}. Points ± S.E. ($n = 4$) are given.

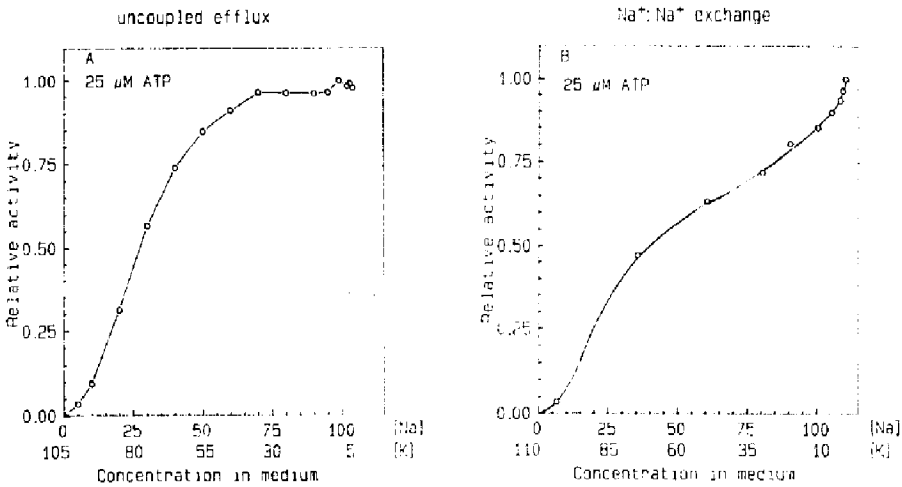

Fig. 2. Typical experiments identical to the one depicted in Fig. 1 but at 25 μM ATP.

exchange, a little less than for Na^+/Na^+ exchange. Hydrolysis accompanying uncoupled Na^+ efflux is activated by cytoplasmic Na^+ along an S-shaped curve with a $K_{0.5}$ of about 4 mM at 1 μM ATP, pH 7.0 (results not shown), i.e., with a comparable $K_{0.5}$ as found for Na^+/Na^+ exchange, which at the same pH has a $K_{0.5}$ of about 6 mM [19]. An ATP concentration of 1 μM is found near-saturating for ATP hydrolysis in reconstituted shark Na^+/K^+-ATPase engaged in uncoupled Na^+ efflux, where a hyperbolic activation by ATP with apparent K_m of 0.20 ± 0.02 μM is found (results not shown). Similar affinities for ATP exist in both the uncoupled Na^+ efflux and the Na^+/Na^+ exchange mode of pump operations, as previously shown for Na^+/Na^+ exchange in both inverted red blood cells [20] and reconstituted shark Na^+/K^+-ATPase [21] and for uncoupled Na^+ efflux in red cells [22].

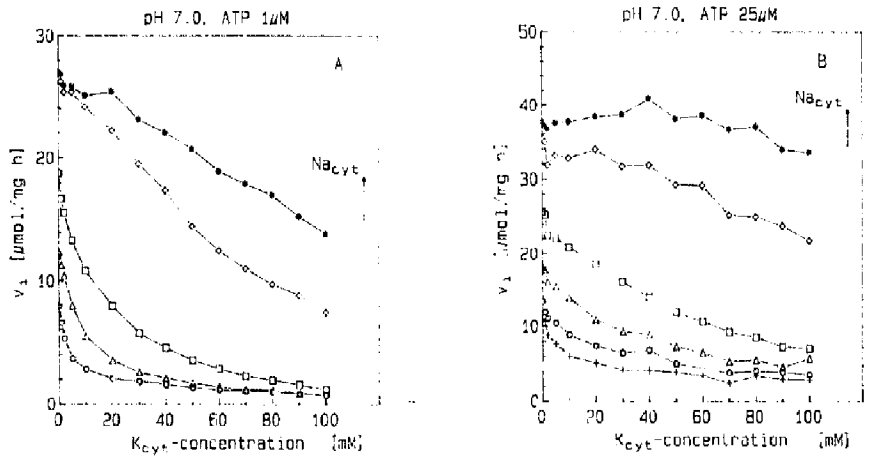

Fig. 3. Typical experiments showing ATP hydrolysis (v_i) accompanying uncoupled Na^+ efflux as a function of K^+_{cyt} concentration at different, fixed cytoplasmic Na^+ concentrations at 1 μM ATP (panel A) and at 25 μM ATP (panel B). The symbols are: (*), 50 mM; (◇), 30 mM; (□), 10 mM; (△), 5 mM; (○), 2 mM; (+), 1 mM. Cytoplasmic Na^+ is replaced isosmotically with sucrose. pH 7.0, 20°C.

The selectivity of the Na^+/K^+-ATPase regarding cytoplasmic Na^+ and K^+ is demonstrated in Figs. 1 and 2 where the effects of inversely varied concentrations of Na^+ and K^+, their sum kept constant, are shown at 1 μM and 25 μM ATP for both uncoupled Na^+ efflux and Na^+/Na^+ exchange. As indicated in these two figures the high-affinity inhibitory effects of K^+_{cyt} in the presence of high Na^+_{cyt} concentrations seen during Na^+/Na^+ exchange (panels 1B and 2B) are absent during the uncoupled mode (panels 1A and 2A) where extracellular Na^+, as well as other alkali cations are omitted. This allows the lower affinity effects of cytoplasmic K^+ to be investigated without interference from the higher affinity K^+_{cyt} inhibition.

The activation curves for the combined action of Na^+ and K^+ as depicted in Figs. 1 and 2 are illustrative of sodium pump selectivity but rather complicated to analyze kinetically due to the concomitantly, reciprocal variation of Na^+ and K^+. Instead, the inhibition pattern of cytoplasmic K^+ during uncoupled Na^+ efflux is investigated at varying cytoplasmic K^+ concentration at different fixed cytoplasmic Na^+ concentrations. The osmolarity is here kept constant by the aid of sucrose. In Fig. 3 a series of such curves are shown at 1 μM ATP (panel A) and at 25 μM ATP (panel B) for cytoplasmic Na^+ fixed at concentrations from 1 mM to 50 mM. When the data at saturating ATP (25 μM) are plotted in a $1/v$ versus K^+_{cyt} plot, an approximately straight line relationship of slope from such plots versus inhibitor concentration (slope replots, not shown) is found for only very limited Na^+ concentrations between 2 and 10 mM and therefore demonstrate

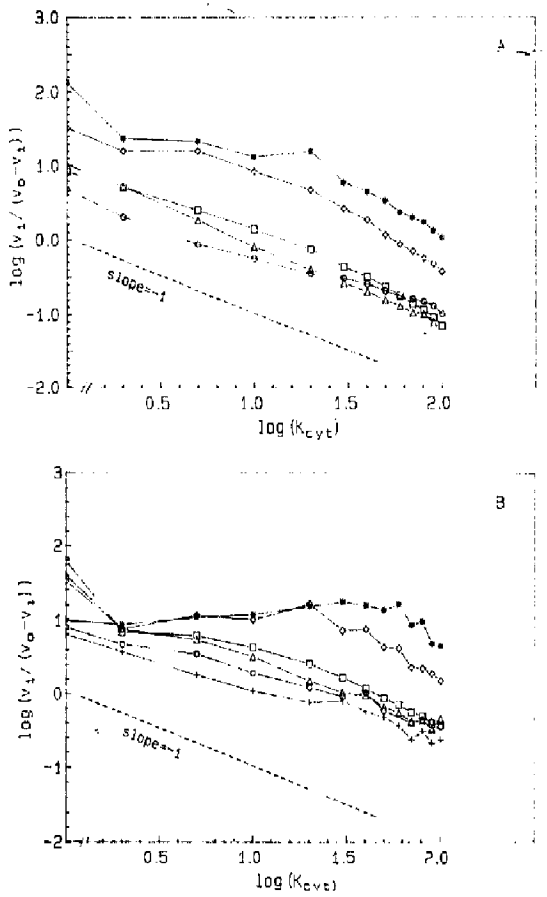

Fig. 4. Replots of the data from Fig. 3 as Hill plots. (A) 1 μM ATP and (B) 25 μM ATP. The symbols are the same as in Fig. 3. To signify the slopes, straight lines with slopes = 1 are presented.

non-linear inhibition by K^+_{cyt} outside this limited interval of Na^+_{cyt}. This indicates that the turnover can be satisfactory described by a velocity equation which contains only first degree terms of the inhibitor concentration, [I], only in this narrow range of Na^+_{cyt}. For higher concentrations of Na^+_{cyt} than 10 mM and less than 2 mM the inhibition is non-linear (i.e., the slope replots are curved), indicating the presence of $[I]^2$ or higher degree [I]-terms in the velocity equation.

The non-linear K^+_{cyt} inhibition as found except outside a very limited range of cytoplasmic Na^+ concentrations, where one K^+_{cyt} inhibitor constant may dominate, makes kinetic analysis using traditional slope replots inaccurate and non-diagnostic for the mechanism of inhibition. Therefore, in order to examine the inhibition pattern over a large range of ligand concentrations (Na^+_{cyt} and K^+_{cyt}), also including the non-linear inhibition part, the model analysis was extended for reasons described below to cover multisite inhibition. In such a system a Hill plot of log $v_i/(v_0 - v_i)$ versus log[I] at different fixed substrate concentrations gives curved lines with limiting slopes of -1 (for $I \to 0$) and $-n_i$ (for $I \to \infty$), in which n_i is the number of inhibitor sites. In this plot v_0 is the velocity at a given fixed Na^+_{cyt} and at zero inhibitor concentration (and not V_{max}), and v_i the velocity at a given concentration of inhibitor. Fig. 4 depicts the Hill plots for the data obtained at 1 μM ATP (panel A) and at 25 μM (panel B). The limiting slopes approach -1 as seen by comparison with indicated straight lines in the figures with slopes of -1.

Effects of pH

Previous results have suggested that at lower pH (pH = 5–6) the relative site affinities for the successive binding of the three Na^+ ions shift in a way such that the affinity for the third Na^+ decreases relative to the binding of the first two, without changing the overall half-maximum activation [6]. If this is correct the pH might also affect the affinity of the multiple inhibitor sites. In Figs. 5A, B the inhibition pattern of K^+_{cyt} inhibition at various fixed Na^+_{cyt} concentrations is depicted at pH 6.0 (panel A) and at pH 8.0 (panel B). The inhibition by K^+_{cyt} at each fixed Na^+_{cyt} concentration is more pronounced at pH 6.0 than at pH 7.0 (compare Figs. 5A and 3A), and as demonstrated in the Hill plot (Fig. 6A) the limiting slope for high K^+_{cyt} concentrations increases at pH 6.0 (approaching -3) relative to pH 7.0 (compare Figs. 4A and 6A).

At pH 8.0 the inhibition pattern is somewhat different in that a plateau for low K^+_{cyt} concentrations appears at the high Na^+_{cyt} concentrations (Fig. 5B). The equivalent Hill plot for K^+_{cyt} inactivation at pH 8.0 is shown in Fig. 6B and demonstrates increased curvature as the concentration of K^+_{cyt} increases (limiting slope approaches -3) compared to the results obtained at lower pH (compare with Figs. 4A and 6A).

Model simulations

In order to arrive at a kinetic model that at least qualitatively describes the inhibition pattern for cytoplasmic K^+ a series of computer simulations were performed for different models of multisite K^+_{cyt} inhibi-

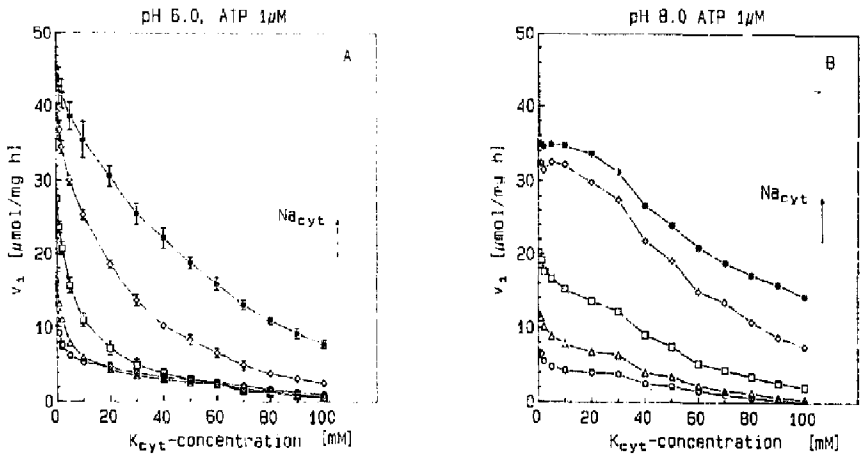

Fig. 5. K^+_{cyt} inhibition of ATP hydrolysis accompanying uncoupled Na^+ efflux at pH 6.0 (A) and at pH 8.0 (B) at different fixed Na^+_{cyt} concentrations (symbols as in Fig. 3). Compare with Fig. 3, which depicts the same type of experiments performed at pH 7.0.

tion. In the light of previously obtained results from red cells that during Na^+/K^+ exchange and K^+/K^+ exchange the three cytoplasmic sites for Na^+ on E_1 are also equally accessible to cytoplasmic K^+ [11,12], it seems appropriate as a first approximation to assume that cytoplasmic K^+ can compete at all three Na^+ sites on E_1A with identical affinities, forming both pure K^+-forms of E_1A and hybrid, Na^+/K^+-forms in which both Na^+ and K^+ are bound to E_1A. The equilibrium species for the proposed model are shown in Table I.

In a previous study of Na^+/Na^+ exchange assuming quasi-equilibrium conditions by which the binding of cations are in rapid equilibrium, and that rate of hydrolysis is proportional to the concentration of bound Na^+, the activation by cytoplasmic Na^+ could be described by a positive cooperative model [19] in which three binding sites on E_1A are successively filled, with intrinsic site dissociation constants of $K_{S1} > K_{S2} = K_{S3}$ at 130 mM extracellular Na^+. Making the same assumptions for uncoupled Na^+ efflux the equation for multisite mixed inhibition with three non-cooperative

TABLE I

Scheme to show possible kinds of enzyme species assuming three sites for both substrate (S) and inhibitor (I)

Enzyme species with either exclusive I, or both I and S bound are assumed kinetically incompetent in the overall reaction.

	ES	ES_2			ES_3		
Competent	S00	SS0			SSS		
	0S0	0SS					
	00S	S0S					
	EI	EI_2 and EIS			EI_3, EI_2S, and EIS_2		
Incompetent	I00	II0	IS0	0SI	III	ISI	SSI
	0I0	0II	SI0	0IS		SII	SIS
	001	I0I	I0S	S0I		IIS	ISS

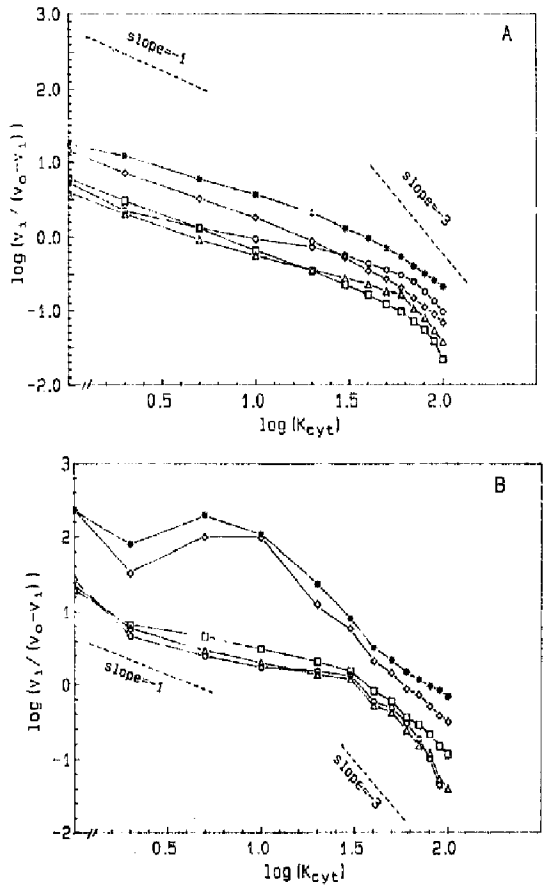

Fig. 6. Replots of the date shown in Figs. 5A, B as Hill plots. Note the increased curvature as $I \to \infty$.

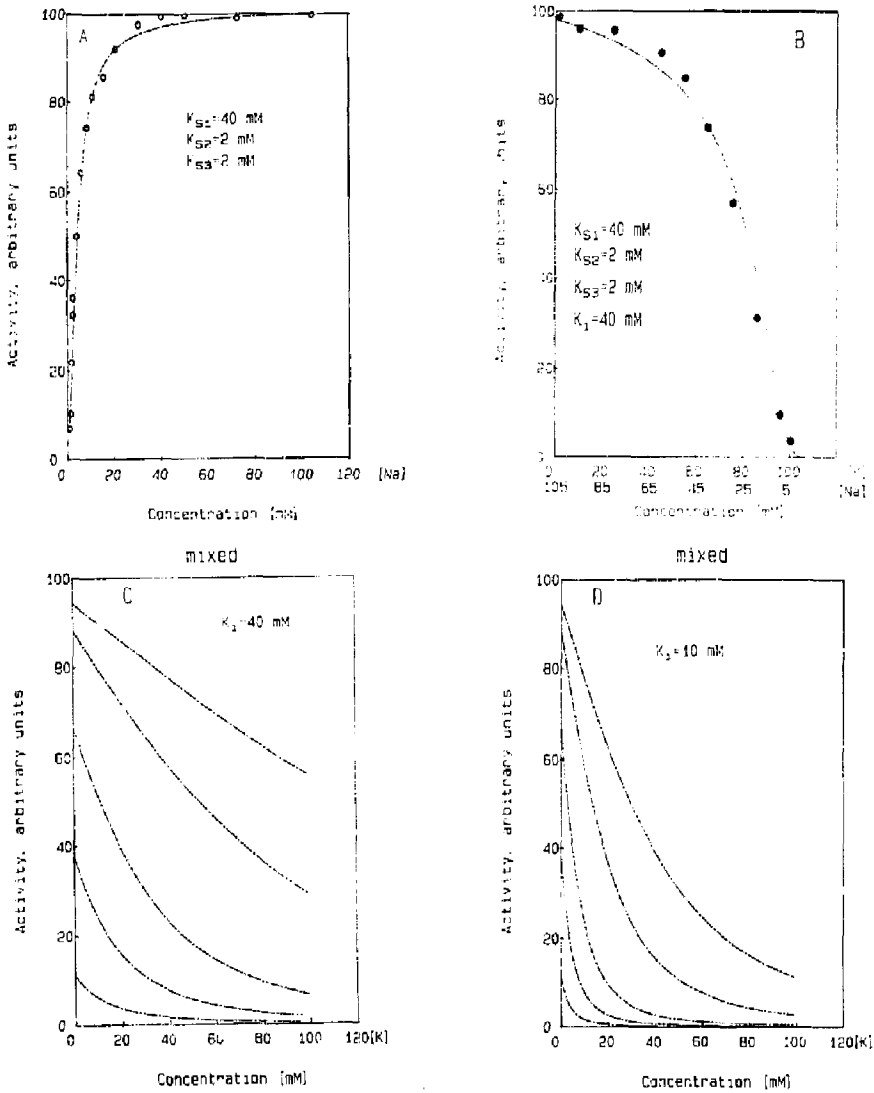

Fig. 7. Model simulations of Na^+_{cyt} activation in the absence of K^+_{cyt} (panel A) and when Na^+ and K^+ are varied reciprocally (panel B), the points shown for comparison are experimental data. Simulation in panel A is to a 3-site cooperative model using the Adair-equation (see below), with K_{S1}, K_{S2}, K_{S3} = 40 mM, 2 mM, 2 mM, setting $K_I = \infty$. Simulations depicted in panel B corresponds to a 3-site mixed inhibition as according to the equation given below with K_I = 40 mM. The K^+_{cyt} inhibition pattern obtained at pH 7.0 at different fixed Na^+ (panel C) where these four site constants are employed should be compared to the data shown in Fig. 3. Panel D simulates the inhibition pattern shown in Fig. 5A obtained at pH 6.0 induced by decreasing K_I to 10 mM. In panel E the inhibition pattern obtained at pH 8.0 are simulated by using a pure competitive model, excluding hybrid binding, with K_I = 40 mM (compare Fig. 5B). In all model simulations, the site constants K_{S1}, K_{S2}, K_{S3} for Na^+_{cyt} binding to E_1A are constant and set to 40 mM, 2 mM, and 2 mM. Note the plateau for small K^+_{cyt} concentrations in panel E as compared to panel C and D. The curves shown are calculated from the following velocity equation as described in the text, with K_I set to infinity for pure Na^+ activation, and Na^+ set to either 2 mM, 5 mM, 10 mM, 30 mM, or 50 mM:

$$\frac{v}{V_{max}} = \frac{\frac{S}{K_{S1}} + \frac{2S^2}{K_{S1}K_{S2}} + \frac{S^3}{K_{S1}K_{S2}K_{S3}}}{1 + \frac{3S}{K_{S1}} + \frac{3S^2}{K_{S1}K_{S2}} + \frac{S^3}{K_{S1}K_{S2}K_{S3}} + \frac{3I}{K_I} + \frac{3I^2}{K_I^2} + \frac{6SI}{K_{S1}K_I} + \frac{3S^2I}{K_{S1}K_{S2}K_I} + \frac{3SI^2}{K_{S1}K_I^2} + \frac{I^3}{K_I^3}}$$

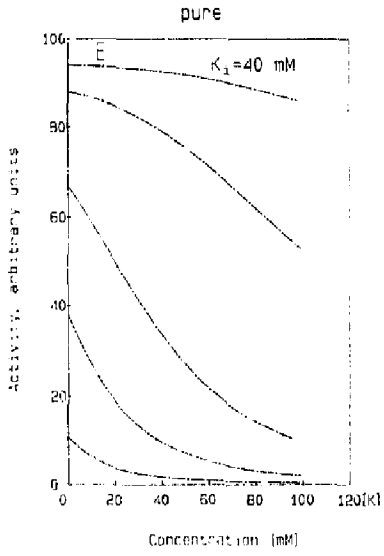

Fig. 7 (continued).

inhibitor site dissociation constants (K_I) and three cooperative substrate sites (K_{S1}, K_{S2}, K_{S3}) is:

$$\frac{v}{V_{max}} = \left(\frac{S}{K_{S1}} + \frac{2S^2}{K_{S1}K_{S2}} + \frac{S^3}{K_{S1}K_{S2}K_{S3}}\right) \times \left(1 + \frac{3S}{K_{S1}} + \frac{3S^2}{K_{S1}K_{S2}} + \frac{S^3}{K_{S1}K_{S2}K_{S3}} + \frac{3I}{K_I} + \frac{3I^2}{K_I^2} + \frac{6SI}{K_{S1}K_I} + \frac{3S^2I}{K_{S1}K_{S2}K_I} + \frac{3SI^2}{K_{S1}K_I^2} + \frac{I^3}{K_I^3}\right)^{-1}$$

It is further assumed in this model that binding of cations are in rapid equilibrium and that turnover of hydrolysis (v) is proportional to fractional saturation of the enzyme (E) with substrate (S, Na^+). This implicitly means that the rate of turnover per binding site is equal, allowing for the possibility of variable stoichiometry as found during some conditions of low Na^+ and pH (Refs. 6 and 23, see Discussion). Binding of inhibitor (I, K^+_{cyt}) to any of the three sites forms a dead-end complex that is kinetically incompetent, i.e., it cannot contribute to hydrolysis (see Table 1). In such a model an increased curvature as $I \to \infty$ shows up in the Hill plot even though cooperativity in the binding of inhibitor is not anticipated. As demonstrated in the Hill plots the slope does increase as the K^+_{cyt} concentrations increases, most clearly observed at pH 6.0 and pH 8.0 (Fig. 6).

Using the velocity equation given above, it is attempted to stimulate the experimentally found inhibition patterns at pH 7.0 at the various fixed Na^+_{cyt} concentrations by assigning proper values for the dissociation constants K_I, K_{S1}, K_{S2}, and K_{S3}. Assuming that the mutual effects of ATP and K^+_{cyt} are solely to displace the equilibrium between the E_1-form and the E_2-form of the enzyme, K_i describing K^+_{cyt} binding to the E_1A-form can be taken to be identical to the constant describing K^+_{cyt} binding to the E_1-form. The intrinsic K^+_{cyt} binding constant to the E_1-form is probably large and has been deduced from work with formycin nucleotides or intrinsic protein fluorescence to be within the range of 5–80 mM [24,25]. As indicated in Figs. 7A and B a reasonable simulation of the experimental data can be obtained for both the pure Na^+ activation (panel 7A) and the combined Na^+/K^+ activation (panel 7B) by assuming site constants for cytoplasmic Na^+ activation of K_{S1} = 40 mM, K_{S2} = 2 mM, and K_{S3} = 2 mM, which are close to the ones previously found for Na^+/Na^+ exchange [19], and an inhibitor constant for cytoplasmic K^+ of K_i = 40 mM. By using these site constants qualitatively quite good simulations of the K^+ inhibition curves at fixed Na^+ are also obtained, compare the calculated curves in Fig. 7C with the experimental curves depicted in Fig. 3. The important point appears to be that K_i must be close to K_{S1} and far from K_{S2} and K_{S3} in order to simulate the experiments and to produce the proper inhibition pattern.

The effects of lowering pH on the inhibition pattern is to increase the relative inhibition of K^+_{cyt} at a given concentration of Na^+_{cyt}, and as seen from the Hill plots, to increase the slope for high inhibitor concentrations. This can be taken to indicate a bringing together of the inhibitor affinity K_i with the affinities for the second and third Na^+_{cyt}, i.e., the pH effects can be accounted for using one and the same model only by modifications of the inhibitor dissociation constant (K_i) for cytoplasmic K^+. Accordingly, by increasing the affinity of K^+_{cyt} by lowering the dissociation constant for cytoplasmic K^+ to 10 mM without affecting the site constants for Na^+_{cyt}, it is possible with the same model to simulate the experimental curves obtained at pH 6.0 (Fig. 7D).

At pH 8.0 the inhibition pattern (Fig. 5B) at the higher Na^+_{cyt} concentrations exhibit a plateau phase for small concentrations of inhibitor, and the relative inhibition by K^+_{cyt} is decreased compared to pH 7.0. This shows that Na^+ protection against K^+ inhibition is enhanced at pH 8.0 and the pattern of inhibition could indicate a pure competitive inhibition, or the affinity of K^+_{cyt} for the ES complexes has decreased to an extent that it cannot be detected in the plots, i.e., at pH 8.0 in the range of Na^+ and K^+ tested, hybrid forms can be assumed no longer to be formed to any appreciable extent. The simulation shows that with pure competi-

tive inhibition good agreements are obtained between experimental and simulated data when K_i is set to 40 mM (Fig. 7E).

Discussion

In the conventional reaction scheme the transition between the two major conformations E_1 and E_2 of the enzyme involves the binding and release of Na^+ and K^+ at the cytoplasmic aspect [26]. In a common interpretation of this scheme the cytoplasmic exchange of Na^+ and K^+ is on the E_1-form which binds Na^+ or K^+ competitively (see, however, Refs. 27 and 28), and the effect of ATP-binding is to accelerate deocclusion of K^+_{cyt}, stabilizing the E_1-form. It does not, however, consider successive binding of Na^+_{cyt} and/or K^+_{cyt}.

Several studies on sided preparations have previously indicated high-affinity K^+ binding presumably at the cytoplasmic surface. A model analysis by Karlish and Stein [15] using reconstituted kidney Na^+/K^+-ATPase lead to the suggestion of high-affinity cytoplasmic K^+ sites with a dissociation constant in the μM area. Van der Hijden and De Pont [16] find both high-affinity and low-affinity K^+_{cyt} inhibition of phosphorylation in reconstituted rabbit kidney Na^+/K^+-ATPase, and suggest that the high-affinity K^+ site are on the E^*-form, a form intermediate between the E_1- and the E_2-form [29,30], whereas the low-affinity inhibition is on the E_2-form. Cornelius and Skou also find both high-affinity and low-affinity K^+_{cyt} inhibition in reconstituted shark Na^+/K^+-ATPase [10] and we suggest that the high-affinity K^+_{cyt} inhibition is through binding to the occluded E_2-form but only when extracellular Cs^+, Li^+, or Na^+ are replacing extracellular K^+.

In the present experiments extracellular K^+ is absent and interference from high-affinity cytoplasmic K^+ inhibition, probably on the enzyme form with occluded K^+-congeners [10], are avoided. Moreover, only Na^+/K^+ competition on the E_1A-form with high affinity for ATP need to be considered, since high concentrations of cytoplasmic K^+ are needed in order to induce the E_2-form: even at 50 mM K^+_{cyt} only high-affinity ATP binding is detected in the ATP substrate curve and about 75 mM K^+_{cyt} must be present to induce the low-affinity ATP binding indicating the presence of the E_2-form [21]. Similar conclusions were also reached from studies in red-cells of Na^+ interaction on K^+/K^+ exchange [12]. During the present conditions the inhibition by cytoplasmic K^+ of ATP hydrolysis accompanying uncoupled Na^+ efflux in the reconstituted Na^+/K^+-ATPase is non-linear, even at very limited concentrations of cytoplasmic Na^+ and the inhibitor dissociation constant is high in accord with fluorescence work [24,25] and with flux-studies from red cells [12], much higher than found in several studies on unsided preparations [13,14,31].

A multisite inhibition model in which K^+_{cyt} competes with three similar site dissociation constants equal to the first site dissociation constant of the three loading sites for cytoplasmic Na^+ is found in principle to describe the present inhibition patterns. In such a model the observed effects of pH on the inhibition patterns can be ascribed to variations in the relative magnitude of K_i (for K^+) compared to K_S (for Na^+). It is not assumed that apparent intrinsic binding constants for cytoplasmic Na^+ and K^+ inferred from steady-state measurements reflect the actual, absolute binding constants in uncoupled Na^+ efflux, which will depend on the actual location of the rate-limiting steps at suboptimal Na^+ concentrations. Since these are believed to be located along the dephosphorylation steps rather than along the Na^+ translocation steps during uncoupled Na^+ efflux and during Na^+/Na^+ exchange it may be conceivable, that steady-state measurements do not give a realistic description of the absolute site dissociation constants, only of their relative variation. On the other hand, equilibrium titration with Na^+ of the eosin fluorescence of membrane bound shark enzyme in the absence of K^+ gives an almost identical sigmoid activation curves as presented here with a $K_{0.5}$ of 4.65 mM (2 μM eosin, pH 7.0: Skou, J.C., personal communication), which is intermediate between the ones found in the present investigation using either uncoupled Na^+ efflux or Na^+/Na^+ exchange.

Several additional mechanisms for cytoplasmic K^+ inhibition were tested in order to evaluate and compare their characteristic inhibition pattern with the experimental data: (a) single site K^+ inhibition is only attainable within a limited range of Na^+_{cyt} and K^+_{cyt}, whereas for higher K^+ concentrations it is clear that non-linear inhibition patterns are encountered. (b) The pure competitive inhibition is not compatible with the inhibition pattern outside very limited K^+ concentrations at pH 7.0, and would give, with $K_i = 40$ mM, a plateau in the inhibition curves at each fixed Na^+ concentration at the lower K^+ concentrations. This is not observed at pH 7.0 and 6.0 (see Figs. 3 and 5A), whereas at pH 8.0 such plateaus are apparent (see Fig. 5B). Therefore, it could be that, e.g., brain and red cell Na^+/K^+-ATPase, exhibit an inhibition pattern more like the shark Na^+/K^+-ATPase at high pH, since, as earlier mentioned, the inhibition pattern of K^+ in these preparations [12,31] could be accommodated by model (a) and/or (b), although the high-affinity K^+ inhibition found in the unsided preparation of brain [31] could speak in favour of a mixed effect where K^+ binds to several enzyme species in the reaction scheme. (c) The partial inhibition in which also enzyme species with hybrid binding of Na^+ and K^+ are kinetically

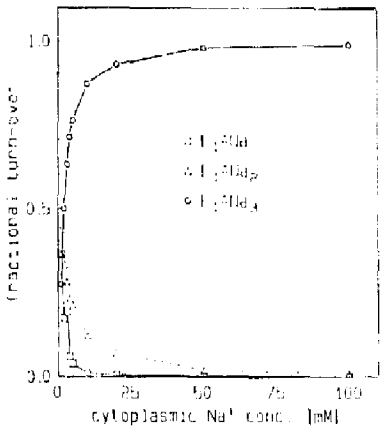

Fig. 8. Calculated turn-over contributed by the enzyme species with one, two, and three Na^+ bound (intrinsic site dissociation constants of K_{S1}, K_{S2}, K_{S3} = 40 mM, 2 mM, and 2 mM) assuming that the turn-over is proportional to the saturation of E_1A with Na^+, which means that the rate per binding site is equal.

competent can be excluded since at high concentrations of K^+ complete inhibition is observed. (d) In the rate equation used enzyme species with 1 and 2 Na^+ can contribute to turn-over in order to accommodate the variable stoichiometry present during special conditions of low Na^+ and pH [6,23], however, with the dissociation constants assigned (K_s) a very small fraction of the enzyme species in the E_1A rapid equilibrium segment will be present with fewer than three bound Na^+ at the Na^+-concentrations high enough to see an effect on the coupling ratio (see Fig. 8).

An important feature of the Na^+/K^+-ATPase is to discriminate between cytoplasmic Na^+ and K^+ [32]. In the present model this discernment is achieved partly by the positive cooperativity exhibited by the binding of the first Na^+_{cyt} ion on successive Na^+ binding [19] as opposed to successive K^+_{cyt} binding, and partly by the kinetically incompetence of hybrid forms. The Na^+/K^+ discrimination is found to be pH dependent and since a downward shift in pH from 7.0 to 5.5 only changes the apparent $K_{0.5}$ for Na^+_{cyt} activation of the uncoupled Na^+ efflux mode from about 4 mM to about 6 mM [6] the quite pronounced effect of pH previously reported on unsided preparations and there ascribed to a cytoplasmic effect [33] seems to indicate either a shift in the inhibitor affinity of K^+ relative to the activation by Na^+ with pH, or that extracellular effects are involved. According to the model presented here the change in cytoplasmic Na^+/K^+ selectivity with pH is caused by different mechanisms at low and high pH: The effect of lowering pH (pH 6.0) can be simulated by an equally increased K^+_{cyt} affinity at all three sites, whereas an increased pH (pH 8.0) seems to increase the selectivity by excluding hybrid binding.

If the interpretation presented is correct it appears that even though the filling of the first binding site takes place with almost identical affinity for cytoplasmic Na^+ and K^+ only the Na^+ binding induces the potentiation in binding affinity for the successive Na^+ binding, and this allosteric (*cis*) effect of the first Na^+ binding enhancing Na^+/K^+ discrimination is potentiated at high pH.

At physiological concentrations of cytoplasmic Na^+ and K^+ (low Na^+, high K^+) and appreciable portion of the enzyme species in the E_1A-pool must be present with bound K^+ and therefore inactive in turnover. This does probably decrease the overall turnover rate during conditions where the rate limiting step in the overall reaction is located to the $E_1A \rightarrow E_2P$ transition, which is probably the case during physiological conditions due to the presence of extracellular K^+ and high ATP [35,36]. Due to this a certain buffer capacity in the turnover of the pump will be present during physiological conditions, and at elevated pH the increased Na^+/K^+ selectivity compensates partially for a decreased turnover which would otherwise results during transient alkaline loads.

Acknowledgements

This work was supported by grants from the Danish Medical Research Council, The Novo Foundation and The Danish Biomembrane Research Centre. I thank Jens G. Nørby and Jens Chr. Skou for helpful comments on the manuscript. The technical assistance of Hanne Zakarias is gratefully acknowledged.

References

1 Garrahan, P.J. and Glynn, I.M. (1967) J. Physiol. Lond. 192, 159–174.
2 Garrahan, P.J. and Glynn, I.M. (1967) J. Physiol. Lond. 192, 175–188.
3 Lew, V.L., Hardy, M.A. and Ellory, J.C. (1976) Biochim. Biophys. Acta 323, 251–266.
4 Glynn, I.M. et al. (1974) Ann. N.Y. Acad. Sci. 242, 257–371.
5 Cornelius, F. (1989) Biochem. Biophys. Res. Commun. 160, 801–807.
6 Cornelius, F. (1990) Biochim. Biophys. Acta 1026, 147–152.
7 Cornelius, F. (1993) in The Sodium Pump: Structure, Mechanism, and Regulation (Kaplan, J.H. and De Weer, P., eds.), pp. 267–280, Rockefeller University Press, New York.
8 Glynn, I.M. (1985) in The Enzymes of Biological Membranes (Martonosi, A.M., ed.), Vol. 3, pp. 35–114, Plenum Press, New York.
9 Cornelius, F. (1991) Biochim. Biophys. Acta 1071, 19–66.
10 Cornelius, F. and Skou, J.C. (1991) Biochim. Biophys. Acta 1067, 227–234.
11 Garay, R.P. and Garrahan, P.J. (1973) J. Physiol. 231, 297–325.
12 Sachs, J.R. (1986) J. Physiol. 374, 221–244.
13 Matsui, H. and Homareda, H. (1982) J. Biochem. 92, 193–217.

14 Jørgensen, P.L. and Petersen, J. (1982) Biochim. Biophys. Acta 765, 38–47.
15 Karlish, S.J.D. and Stein, W.D. (1985) J. Physiol. Lond. 359, 119–149.
16 Van der Hijden, H.T.W.M. and De Pont, J.J.H.H.M. (1989) Biochim. Biophys. Acta 983, 142–152.
17 Cornelius, F. (1988) Methods Enzymol. 156, 156–167.
18 Cornelius, F. and Skou, J.C. (1984) Biochim. Biophys. Acta 772, 357–373.
19 Cornelius, F. and Skou, J.C. (1988) Biochim. Biophys. Acta 944, 223–232.
20 Blostein, R. (1983) J. Biol. Chem. 258, 7948–7953.
21 Cornelius, F. and Skou, J.C. (1987) Biochim. Biophys. Acta 904, 353–364.
22 Glynn, I.M. and Karlish, S.J.D. (1976) J. Physiol. 256, 465–496.
23 Polvani, C. and Blostein, R. (1988) J. Biol. Chem. 263, 16757–16763.
24 Beaugé, L.A. and Glynn, I.M. (1980) J. Physiol. 299, 367–383.
25 Karlish, S.J.D. (1980) J. Bioenerg. Biomembr. 12, 111–136.
26 Karlish, S.J.D., Yates, D.W. and Glynn, I.M. (1978) Biochim. Biophys. Acta 525, 252–264.
27 Skou, J.C. and Esmann, M. (1983) Biochim. Biophys. Acta 746, 101–113.
28 Esmann, M. and Skou, J.C. (1983) Biochim. Biophys. Acta 748, 413–417.
29 Nørby, J.G., Klodos, I. and Christiansen, N.O. (1983) J. Gen. Physiol. 82, 725–758.
30 Yoda, S. and Yoda, A. (1986) J. Biol. Chem. 261, 1147–1152.
31 Plesner, L. and Plesner, I.W. (1985) Biochim. Biophys. Acta 818, 222–234.
32 Skou, J.C. (1983) Curr. Top. Membr. Transp. 19, 323–341.
33 Skou, J.C. and Esmann, M. (1980) Biochim. Biophys. Acta 601, 386–402.
34 Shani-Sekler, M., Goldshleger, R., Tal, D.M. and Karlish, S.J.D. (1988) J. Biol. Chem. 263, 19331–19341.
35 Forbush, B., III (1987) J. Biol. Chem. 262, 11104–11115.
36 Skou, J.C. (1991) in The Sodium Pump: Recent Developments (Kaplan, J.H. and De Weer, P., eds.), pp. 313–316, The Rockefeller University Press, New York.